Journal of Dental Sciences 19 (2024) 2268–2277

Available online at www.sciencedirect.com

ScienceDirect

journal homepage: www.e-jds.com

Original Article

Rho GTPase activating protein 11A promotes tongue squamous cell carcinoma proliferation and is a transcriptional target of forkhead box M1

Weiwei Zhang [a], Xueyan Bai [a], Tingting Liu [b], Yulong Mao [c], Lingnan Zhang [a], Wenlong Wang [c], Huanying Yu [d*]

[a] *Department of Orthodontics, Binzhou Medical University Hospital, Binzhou, China*
[b] *Department of Oral Medicine, Binzhou Medical University Hospital, Binzhou, China*
[c] *Department of Oral and Maxillofacial Surgery, Binzhou Medical University Hospital, Binzhou, China*
[d] *Department of Prosthodontics, Binzhou Medical University Hospital, Binzhou, China*

Received 7 January 2024; Final revision received 16 February 2024
Available online 29 February 2024

KEYWORDS
ARHGAP11A;
FOXM1;
Tongue squamous cell carcinoma;
Cell cycle

Abstract *Background/purpose:* Rho GTPase activating protein 11A (ARHGAP11A) can facilitate GTP hydrolysis in RhoA. The functions of ARHGAP11A in oral squamous cell carcinoma (OSCC) have not yet been explored. This study aimed to investigate the expression profile of ARHGAP11A in OSCC, its correlation with patient prognosis, its effect on cell-cycle progression, and the mechanisms by which it is dysregulated.
Materials and methods: Bioinformatics analysis was conducted using data from The Cancer Genome Atlas-Head and Neck Squamous Cell Carcinoma (TCGA-HNSC). Lentiviruses carrying *ARHGAP11A* shRNAs were employed to determine the effects of *ARHGAP11A* knockdown on tumor cell proliferation and cell-cycle progression. Dual-luciferase reporter assays were utilized to examine how FOXM1 transcriptionally regulates *ARHGAP11A* expression.
Results: ARHGAP11A upregulation was associated with unfavorable overall survival (OS) in patients with TSCC (HR: 2.142, 95%CI: 1.224–3.749, $P = 0.007$), but not in patients with OSCC of sites other than the tongue. *ARHGAP11A* knockdown inhibited the proliferation of TSCC cells *in vitro* and *in vivo*, and induced G1 phase arrest. *ARHGAP11A* knockdown increased GTP-RhoA but decreased p-RB levels, while it did not affect the total expression of RhoA and RB. *ARHGAP11A* knockdown increased p27 and decreased cyclin E1 expression. *ARHGAP11A* is transcriptionally activated by FOXM1 via multiple FOXM1 binding sites in the promoter regions in TSCC cells.
Conclusion: This study revealed the oncogenic role of ARHGAP11A in TSCC, highlighting its impact on cell-cycle control and tumor proliferation. Furthermore, the regulatory

* Corresponding author. Department of Prosthodontics, Binzhou Medical University Hospital, No. 661, Huanghe 2nd Road, Binzhou City, Shandong Province, 256603, China.
E-mail address: yuhuanying56@163.com (H. Yu).

https://doi.org/10.1016/j.jds.2024.02.015

relationship between FOXM1 and ARHGAP11A provides new insights into the transcriptional networks in TSCC.

Introduction

Head and neck squamous cell carcinoma (HNSCC) encompasses a diverse group of cancers that arise from the mucosal surfaces within the head and neck region.[1] The disease exhibits anatomic heterogeneity, as tumors can originate from a variety of locations including the oral cavity, oropharynx, larynx, and hypopharynx.[2] Differences in risk factors, molecular profiles, and response to therapies have been seen among HNSCC arising from differing anatomical sites.[1,3] Consequently, there is an increasing recognition of the necessity to study HNSCC subtypes based on their specific anatomical origins, rather than considering them as a homogeneous group.

Small GTPases of the Rho family function as intracellular signaling molecules that control key cellular processes, including migration, polarity, and cell cycle progression.[4] When bound to GTP, these proteins are activated to modulate a series of downstream pathways. Rho GTPases have been implicated in cancer development, usually through aberrant expression or activation.[5,6] The control of the alternating states, active GTP-bound and inactive GDP-bound, in Rho proteins involves three distinct protein types. Rho-specific guanine nucleotide exchange factors (Rho GEFs) play a role in facilitating the transition of these GTPases into their active form by replacing GDP with GTP. On the other hand, GTPase-activating proteins (Rho GAPs) stimulate the intrinsic GTPase activity of Rho GTPase proteins, leading to the conversion of the active GTP-bound state to the inactive GDP-bound state. Additionally, guanine nucleotide dissociation inhibitors (Rho GDIs) are involved in regulating this process.[6]

ARHGAP11A is a Rho GAP and catalyzes the GTP hydrolysis of RhoA.[5,7] Its overexpression was associated with enhanced proliferation and invasion of basal-like breast cancer,[5] colon cancer,[7] hepatocellular carcinoma.[8] Its overexpression was linked to poor prognosis in lung adenocarcinoma,[9] and gastric cancer.[10] However, its functional regulations in oral squamous cell carcinoma (OSCC) have not been studied yet. This study focuses on the expression profile of *ARHGAP11A* and its association with prognosis in the subtypes of OSCC, its regulation of cell-cycle progression, and the mechanisms leading to its aberrant upregulation.

Materials and methods

Bioinformatics analysis

The TCGA-HNSC dataset, which includes gene expression and survival data, was retrieved from the UCSC Xena browser (https://xenabrowser.net/).[11] Anatomic site information for each case was extracted, and cases of oral squamous cell carcinoma were isolated by excluding those related to the nasopharynx, oropharynx, and larynx. Cell-cycle dependent ARHGAP11A expression was checked using data from the Human Protein Atlas (https://www.proteinatlas.org/).[12] The fluorescent ubiquitination-based cell cycle indicator (FUCCI) staining system has been well-characterized in U2OS cells in the HPA database, providing a reliable and validated model for cell cycle studies. Their robust proliferative capacity and clear cell cycle phase transitions make U2OS an ideal choice for monitoring cell cycle perturbations.[13]

Immunohistochemistry (IHC) staining

Commercial HNSCC tissue microarrays (XHN803) containing tumors from tongue were obtained from Taibsbio (Xi'an, China) were deparaffinized and subjected to heat-induced antigen retrieval. Slides were stained on the BOND-III Automated IHC Stainer (Leica, Wetzlar, Germany) using a rabbit anti-ARHGAP11A polyclonal primary antibody (PA5-59170, ThermoFisher, Waltham, MA, USA) at a 1:200 dilution for 15 min. Slides were then counterstained with hematoxylin.

Cell culture and treatment

The OSCC cell lines SCC4 and SCC25 were acquired from Procell (Wuhan, China) and cultured under the recommended medium and conditions. Recombinant lentiviruses for *ARHGAP11A* or *FOXM1* knockdown were generated using pLKO.1-puro to express the following shRNAs: shARHGAP11A#1, 5′-GCTATCTGAATCACCAGTGAT-3'; shARHGAP11A#2, 5′-CGGTATCAGTTCACATCGATA-3'; shFOXM1#1, 5′-GCCCAACAGGAGTCTAATCAA-3′, shFOXM1#2, 5′-GCCAATCGTTCTCTGACAGAA-3′, scramble control, 5′-CCTAAGGTTAAGTCGCCCTCG-3'. Recombinant lentiviruses were produced by transfecting DNA mixture containing 9 μg of pLKO.1-puro, 6.5 μg of psPAX2, and 3.5 μg of pMD2.G into HEK 293T cells in a 10 cm culture dish. The virus-containing supernatant was collected 48 h after infection.

Reverse transcription quantitative PCR

RNA extraction and the subsequent reverse transcription quantitative PCR (RT-qPCR) was performed following a method introduced previously.[14] Relative gene expression was calculated using the $2^{-\Delta\Delta Ct}$ method by normalizing to *ACTB* levels. The following primers were used for amplification: *ARHGAP11A,* forward, 5′-GAAGCTACGATTACAGGCTGCAG-3′,

reverse, 5′- CCTTCCAGTGATGGAGTAGCAC-3'; *FOXM1*, forward, 5′-TCTGCCAATGGCAAGGTCTCCT-3′, reverse, 5′-CTGGATTCGGTCGTTTCTGCTG-3'; and *ACTB*, forward, 5′-CACCATTGGCAATGAGCGGTTC-3′, reverse, 5′-AGGTCTTT GCGGATGTCCACGT-3'.

Western blotting assays

Cells were harvested and lysed in RIPA buffer containing protease and phosphatase inhibitors (P0013B, Beyotime, Shanghai, China). The protein concentration was determined using a BCA assay kit (P0010S, Beyotime). Proteins were then separated on SDS-PAGE gels and transferred onto nitrocellulose membranes. The membranes were blocked and incubated with a primary antibody specifically targets ARHGAP11A (1:1000, PA5-59170, ThermoFisher Scientific), FOXM1 (1:1000, #5436, Cell Signaling Technology, Danvers, MA, USA), GTP-RhoA (1:1000, 26904, NewEast Biosciences, Prussia, PA, USA), p-RB (1:1000, #8516, Cell Signaling Technology), RB (1:1000, #9309, Cell Signaling Technology), p27 (1:2000, 25614-1-AP, Proteintech), cyclin D1 (1:5000, 26939-1-AP, Proteintech), cyclin E1 (1:1000, 11554-1-AP, Proteintech), or β-actin (1:1000, #9562, Cell Signaling Technology) overnight at 4 °C. After thoroughly washing, the membranes were incubated with horseradish peroxidase (HRP)-conjugated secondary antibodies appropriate for either rabbit or mouse primary antibodies. The protein bands were visualized using an enhanced chemiluminescence (ECL) reagent and captured on a digital imaging system.

Cell proliferation assays *in vitro*

To evaluate cell proliferation, experiments involving the Cell Counting Kit-8 (CCK-8) and colony formation assays were conducted, following the methods introduced previously.[15]

Transwell migration and invasion assays

Migration and invasion assays were conducted using Transwell chambers with 8.0 μm pore polycarbonate membrane inserts (8 μm PET membrane, #3464, Corning, Corning, NY, USA) (for migration) and Matrigel-coated inserts (200 μg/mL for invasion) in 24-well plates. For migration assays, 5×10^4 cells were seeded into the upper chamber in serum-free medium. The lower chamber was filled with medium containing 10% FBS as a chemoattractant. After 24 h of incubation, cells that had migrated through the membrane were fixed, stained with crystal violet, and counted under a microscope. For invasion assays, the procedure was similar, except that the cells were seeded into Matrigel-coated inserts and incubated for 48 h. Each assay was performed in triplicate.

Animal studies

The animal experiments were reviewed and approved by the Institutional Animal Care and Use Committee (IACUC) of Binzhou Medical University Hospital and were conducted at the Jinruijie Biotechnology Service Center, Chengdu, China (ethical approval no. JRJ20230316). All procedures adhered to the methods described previously,[15] in accordance with the Institutional Guide for the Care and Use of Laboratory Animals, as well as the ARRIVE Guidelines.[16] Six-week-old nude mice, obtained from Vital River Laboratory Animal Technology (Beijing, China), were utilized for the *in vivo* studies. 3×10^6 SCC4 and SCC25 cells, either with or without *ARHGAP11A* knockdown, were suspended as a single-cell solution in 100 μl of a 1:1 mixture of PBS and Matrigel. This cell suspension was then injected into the subcutaneous tissue of the mice. After 35 days, euthanasia was humanely performed by carbon dioxide inhalation. The tumors were then harvested to assess their weight and to perform immunohistochemical analysis of the Ki-67 proliferation marker.

Flow cytometric analysis

Flow cytometric analysis of cell-cycle distribution was performed following a standard protocol using propidium iodide (PI).[17] In brief, two days post-lentiviral transduction, the cells were collected, washed by PBS, fixed in 70% ethanol, permeabilized and stained with a propidium iodide (PI) staining solution containing RNase A. The stained cells are analyzed using a FACSymphony A3 flow cytometer (BD Biosciences, Franklin Lakes, NJ, USA). The cell-cycle distribution is analyzed using NovoExpress (v1.5.7, Agilent, Santa Clara, CA, USA) software.

Dual-luciferase reporter assay

The *ARHGAP11A* gene promoter sequences (Supplementary Fig. 1) were scanned using the Jaspar database to explore the potential binding site.[18] Then, the integrated or truncated promoter segments were synthesized and inserted into the multiple cloning sites in pGL3-basic luciferase reporter vector. SCC4 or SCC25 cells with or without lentivirus-mediated *ARHGAP11A* knockdown were seeded in 24-well plates, and allowed to reach about 70% confluency. Then, the cells were co-transfected with 0.75 μg of recombined pGL3 plasmids, along with 0.025 μg of pRL-TK for normalization. 48 hrs later, luciferase activity was measured using a luminometer and a dual-luciferase assay kit (Promega).

Statistical analysis

The data were compiled and statistically analyzed using GraphPad Prism software (version 9.5.1) (GraphPad Software, San Diego, CA, USA). Data were reported as mean ± SD ($n = 3$). Univariate and multivariate Cox proportional hazards regression analyses were performed to assess the association between *ARHGAP11A* expression and OS in patients with OSCC. The parameters with $P < 0.1$ in univariate analysis were included in multivariate analysis. For comparisons between two groups, the unpaired Welch's t-test was utilized, while comparisons among multiple groups were conducted using Analysis of Variance (ANOVA) with a Tukey post-hoc test for multiple comparisons. Pearson's r values were calculated to estimate the correlations. $P < 0.05$ was considered statistically significant.

Results

ARHGAP11A upregulation is associated with poor prognosis in tongue squamous cell carcinoma

Given that OSCC can originate from various anatomical sites within the oral cavity, we further investigated its expression across these different sites and confirmed significant heterogeneity (Fig. 1B, One-way ANOVA $P < 0.001$). We focused on TSCC as the predominant subtype of OSCC. Subgroup analysis revealed a significant increase in *ARHGAP11A* expression within TSCC (Fig. 1C). The key clinicopathological parameters between primary TSCC cases with high and low *ARHGAP11A* expression were compared in Table 1. No significant difference was observed in these parameters. No survival difference was observed in overall survival (OS) and progression-free interval (PFI) when primary OSCC cases were stratified by median *ARHGAP11A* expression (Fig. 1D). However, further analysis indicated that in primary TSCC cases, the group with higher *ARHGAP11A* expression had a significantly worse OS compared to the group with lower expression (HR: 2.142, 95%CI: 1.224–3.749, $P = 0.007$) (Fig. 1E). Multivariate analysis showed that higher *ARHGAP11A* expression is an independent indicator of unfavorable OS, after adjusting for pathological stages (HR: 2.319, 95%CI: 1.290–4.159, $P = 0.005$) (Table 2). Immunohistochemistry (IHC) assays were then conducted using a commercial tissue microarray containing 24 TSCC and 3 tumor adjacent normal tissues. Results confirmed positive ARHGAP11A staining in OSCC but not in adjacent normal tissues (Fig. 1F and G). Additionally, cell line-based RNA-sequencing data from Cancer Cell Line Encyclopedia (CCLE) (https://sites.broadinstitute.org/ccle/)[19] showed that the TSCC cell lines usually have high *ARHGAP11A* expression (Fig. 1H).

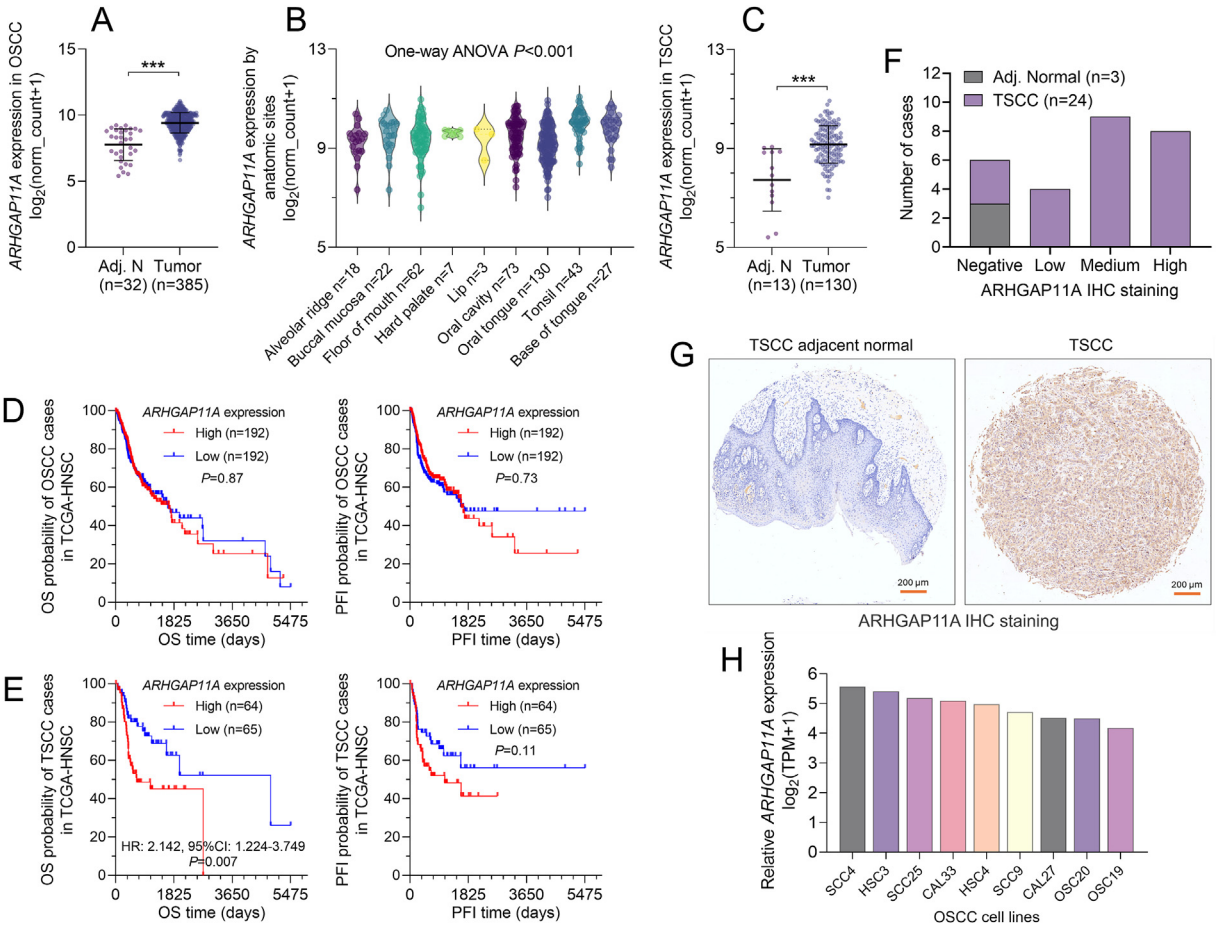

Figure 1 *ARHGAP11A* upregulation was associated with poor prognosis in tongue squamous cell carcinoma. **A.** Comparison of *ARHGAP11A* between primary oral squamous cell carcinoma (OSCC) tissues and adjacent normal tissues in The Cancer Genome Atlas-Head and Neck Squamous Cell Carcinoma (TCGA-HNSC). **B.** Comparison of *ARHGAP11A* expression in primary tumors from different anatomic sites in TCGA-HNSC. **C.** Comparison of *ARHGAP11A* between primary tongue squamous cell carcinoma (TSCC) tissues and adjacent normal tissues in TCGA-HNSC. **D-E.** Patients with primary OSCC (D) or tongue squamous cell carcinoma (TSCC) (E) were separated into two groups by median *ARHGAP11A* expression. Kaplan–Meier (K–M) survival curves were generated to compare the difference in overall survival (OS) and progression-free survival (PFI) between the higher and lower *ARHGAP11A* expression group. **F-G.** Quantitative results (F) and representative images (G) of immunohistochemistry (IHC) staining of ARHGAP11A in TSCC tumor tissues and adjacent normal tissues of a commercial TSCC tissue microarray. **H.** *ARHGAP11A* mRNA expression in multiple TSCC cell lines, using from data from Cancer Cell Line Encyclopedia (CCLE).

Table 1 Comparison of key clinicopathological parameters between primary TSCC cases with high and low *ARHGAP11A* expression.

Characteristics	*ARHGAP11A* expression		Total (N = 129)	*P* value
	High (N = 64)	Low (N = 65)		
OS status				
0	33 (25.58%)	46 (35.66%)	79 (61.24%)	0.03
1	31 (24.03%)	19 (14.73%)	50 (38.76%)	
Pathological stages				
I and II	19 (16.10%)	16 (13.56%)	35 (29.66%)	0.69
III and IV	40 (33.90%)	43 (36.44%)	83 (70.34%)	
Gender				
Female	24 (18.60%)	22 (17.05%)	46 (35.66%)	0.72
Male	40 (31.01%)	43 (33.33%)	83 (64.34%)	
Histologic Grade				
G1	5 (3.88%)	12 (9.30%)	17 (13.18%)	0.22
G2	46 (35.66%)	42 (32.56%)	88 (68.22%)	
G3	13 (10.08%)	11 (8.53%)	24 (18.60%)	
Age at initial pathologic diagnosis				
Mean ± SD	58.45 ± 13.26	57.32 ± 13.88	57.88 ± 13.53	
Tobacco smoking history				
1	22 (17.46%)	25 (19.84%)	47 (37.30%)	0.08
2	20 (15.87%)	17 (13.49%)	37 (29.37%)	
3	4 (3.17%)	12 (9.52%)	16 (12.70%)	
4	17 (13.49%)	9 (7.14%)	26 (20.63%)	
Margin status				
Close	8 (6.45%)	5 (4.03%)	13 (10.48%)	0.11
Negative	54 (43.55%)	50 (40.32%)	104 (83.87%)	
Positive	1 (0.81%)	6 (4.84%)	7 (5.65%)	

OS: overall survival. SD: standard deviation.Tobacco smoking history: 1: Lifelong Non-Smoker; 2: Current Smoker; 3: Former Smoker; 4: Current Reformed Smoker for >15 years.

Table 2 Univariate and multivariate analysis of the parameters related to overall survival.

	Univariate analysis				Multivariate analysis			
	P value	HR	95%CI		*P* value	HR	95%CI	
Age at initial pathologic diagnosis	0.461	1.009	0.985	1.033				
Gender								
Female (n = 46)	0.713	1.115	0.625	1.990				
Male (n = 83)		1.000						
***ARHGAP11A* expression**								
High (n = 64)	0.008	2.196	1.226	3.935	0.005	2.316	1.290	4.157
Low (n = 65)		1.000						
Margin status								
Close (n = 13)	0.889	0.903	0.216	3.771				
Negative (n = 104)	0.820	0.883	0.303	2.576				
Positive (n = 7)		1.000						
Pathological stages								
I/II (n = 35)	0.077	0.516	0.247	1.075	0.051	0.480	0.230	1.002
III/IV (n = 83)		1.000						
Tobacco smoking history								
1 (n = 47)	0.121	0.523	0.231	1.186				
2 (n = 37)	0.391	1.381	0.660	2.889				
3 (n = 16)	0.656	0.800	0.300	2.133				
4 (n = 26)		1.000						
Histological grade								
G1 (n = 17)	0.178	0.462	0.15	1.422				
G2 (n = 88)	0.406	0.758	0.394	1.458				
G3 (n = 24)		1.000						

Knocking down of *ARHGAP11A* expression impairs the proliferation of tongue squamous cell carcinoma

Considering the typically high *ARHGAP11A* expression in TSCC cell lines, we utilized two such lines available in our laboratory, SCC4 and SCC25, for functional validation. Both cell lines were transduced with recombinant lentivirus to achieve *ARHGAP11A* knockdown (Fig. 2A and B). The knockdown of *ARHGAP11A* significantly reduced the viability, proliferation, migration, and invasion of these cell lines (Fig. 2C–E). In xenograft tumor models, *ARHGAP11A* knockdown also markedly decreased tumor growth *in vivo* (Fig. 2F and G). IHC staining showed a reduced percentage of Ki-67-positive cells in the *ARHGAP11A* knockdown group compared to the scramble control group (Fig. 2H).

ARHGAP11A knockdown induces G1 phase arrest by regulating multiple cell-cycle proteins in tongue squamous cell carcinoma

ARHGAP11A expression and its regulation on RhoA activity are cell-cycle dependent in colon cancer.[7] Our review of fluorescent ubiquitination-based cell cycle indicator (FUCCI) staining data from the Human Protein Atlas (HPA) revealed that cells in the G2/M phase (Geminin-positive) exhibited stronger ARHGAP11A staining compared to those in the G1 phase (CDT1-positive) (Fig. 3A). Quantitative results indicated that both *ARHGAP11A* mRNA and protein expression peak in the G2/M phase (Fig. 3B). Western blot assays revealed that *ARHGAP11A* knockdown increased GTP-RhoA levels but

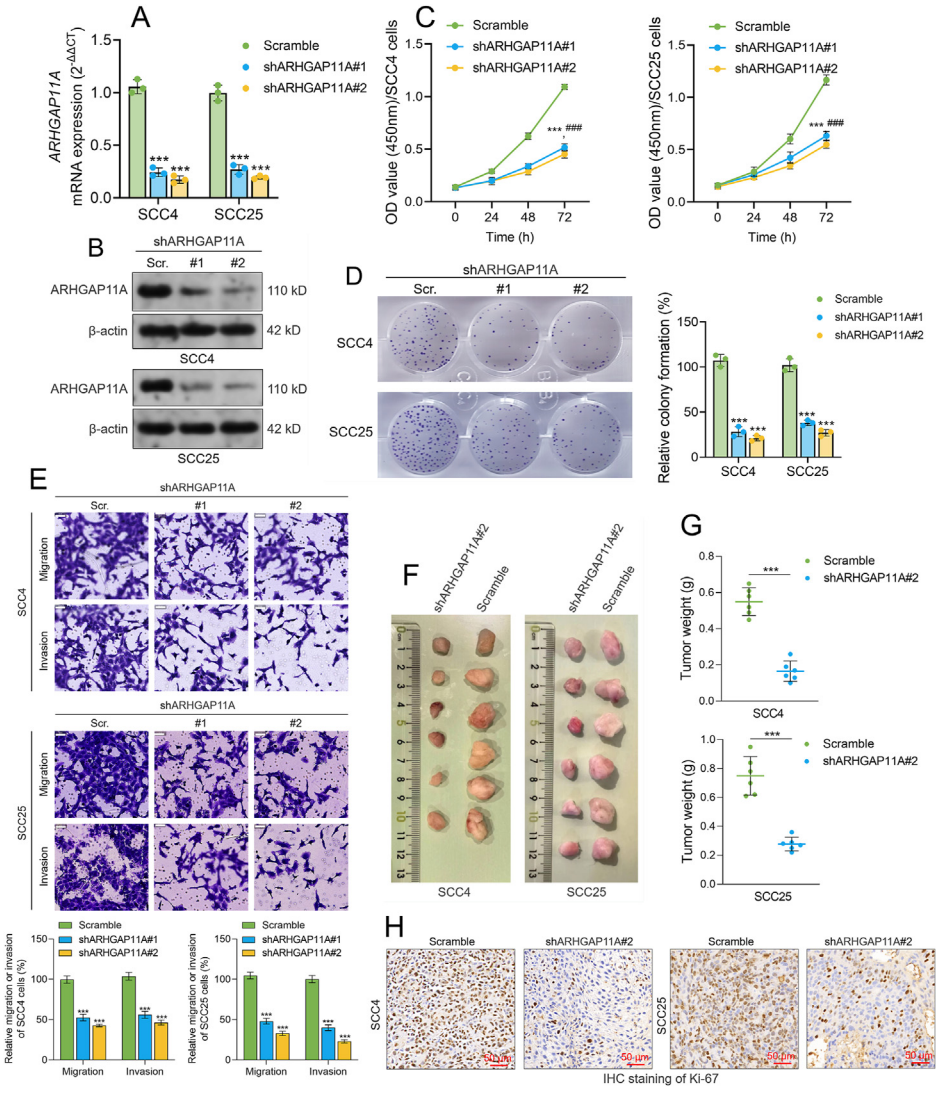

Figure 2 Knocking down of *ARHGAP11A* expression impairs the proliferation of tongue squamous cell carcinoma. **A-B.** RT-qPCR and western blotting analyses were performed to check the expression of *ARHGAP11A* at the mRNA (A) and protein (B) levels in SCC4 and SCC25 cells 48 h after lentivirus-mediated *ARHGAP11A* knockdown. **C-E.** CCK-8 (C), colony formation (D) and transwell assay of migration and invasion (E) were performed to explore the influence of *ARHGAP11A* knockdown on cell proliferation, migration and invasion in SCC4 and SCC25 cells. **F-G.** SCC4 and SCC25 cells with or without lentivirus-mediated *ARHGAP11A* knockdown were used for *in vivo* studies. Xenograft tumors were removed and pictured (E) and the weights of tumors in each group (F) were calculated at the end of animal study. **H.** Representative immunohistochemistry (IHC) staining images of Ki-67 expression SCC4- and SCC25-derived xenograft tumors. Scale bar: 50 μm $^{\#\#\#}$ and ***, $P < 0.001$.

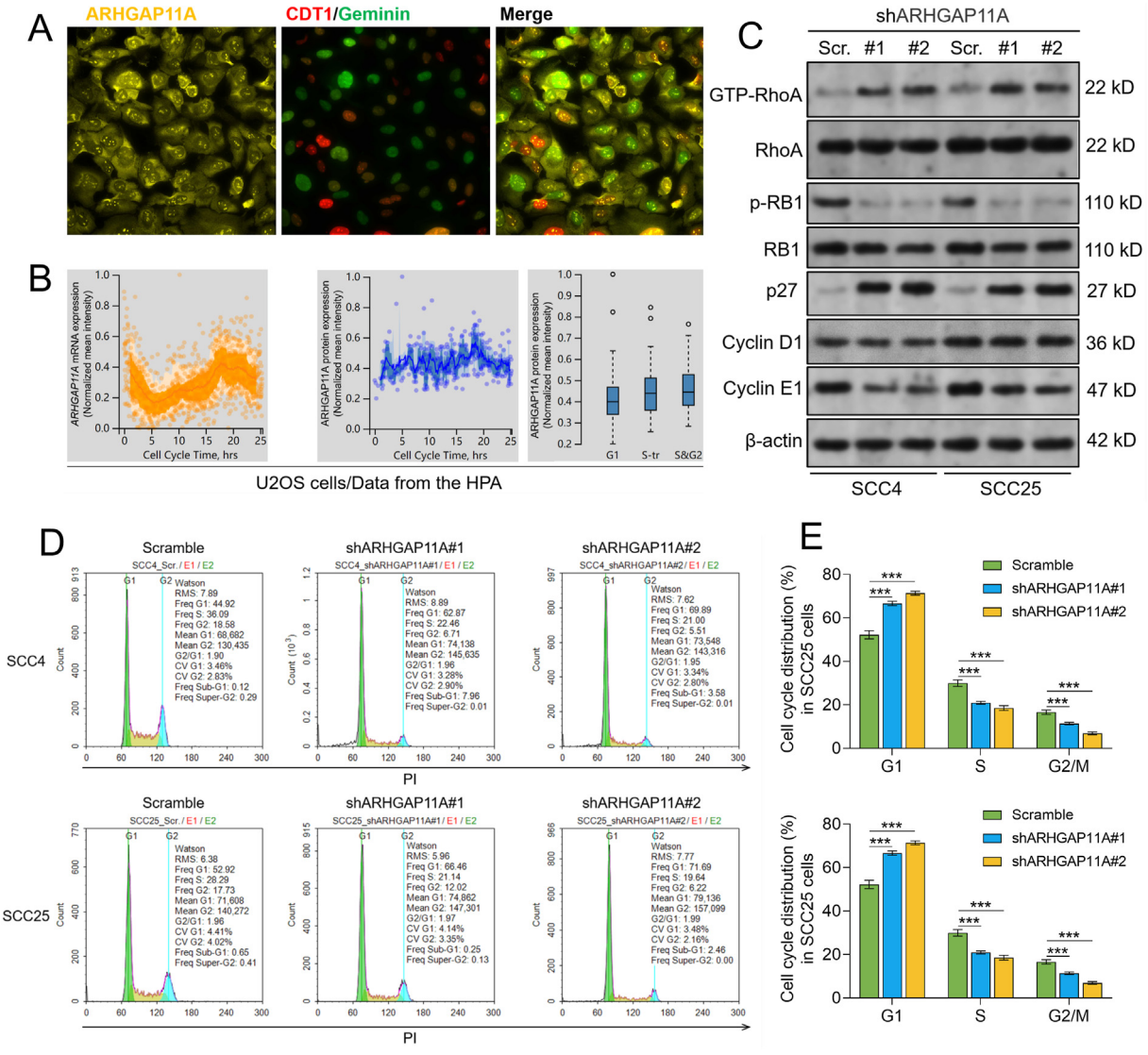

Figure 3 *ARHGAP11A* knockdown induces G1 phase arrest by regulating multiple cell-cycle proteins in tongue squamous cell carcinoma. **A-B.** Representative fluorescent ubiquitination-based cell cycle indicator (FUCCI) images and ARHGAP11A staining (A) and quantitation of *ARHGAP11A* mRNA and protein expression in different phases with the cell-cycle (B) in U2OS cells in the human protein atlas (HPA). Image credit: the HPA, data were retrieved from: https://www.proteinatlas.org/ENSG00000198826-ARHGAP11A/subcellular#cell_cycle. **C.** Western blotting analysis was performed to check the expression of indicated proteins in SCC4 and SCC25 cells 48 h after lentivirus-mediated *ARHGAP11A* knockdown. **D-E.** Representative images (D) and quantitation (E) of cell-cycle distribution of SCC4 and SCC25 cells with or without lentivirus-mediated *ARHGAP11A* knockdown. ***, $P < 0.001$.

reduced phosphorylated RB (p-RB) levels, without affecting total RhoA and RB expression (Fig. 3C). Additionally, *ARHGAP11A* knockdown caused an upregulation of p27 and a downregulation of cyclin E1 expression (Fig. 3C). Flow cytometry analysis showed that *ARHGAP11A* knockdown induced a higher rate of G1 phase arrest in both SCC4 and SCC25 cells (Fig. 3D and E).

ARHGAP11A is transcriptionally activated by FOXM1 in tongue squamous cell carcinoma cells

Given the transcriptional overactivation of *ARHGAP11A* in TSCC, we investigated potential transcription factors (TFs) that could regulate its expression. We identified candidate TFs and chromatin regulators that may bind to the ARHGAP11A promoter region (within 10 kb upstream of the transcription start site) using the Cistrome Data Browser (http://cistrome.org/db/#/).[20] We then examined the correlation between *ARHGAP11A* expression and the expressions of the 72 candidate genes (Fig. 4A; Supplementary Table 1) in a cohort of 130 primary TSCC patients from the TCGA-HNSC database. Detailed Pearson's correlation coefficients are provided in Supplementary Table 1. This analysis identified *FOXM1* as the gene most significantly correlated with *ARHGAP11A*, exhibiting a strong positive correlation ($r = 0.72$) (Fig. 4B). Moreover, *FOXM1* knockdown in SCC4 and SCC25 cells resulted in a considerable decrease in *ARHGAP11A* expression at both mRNA and protein levels (Fig. 4C—E).

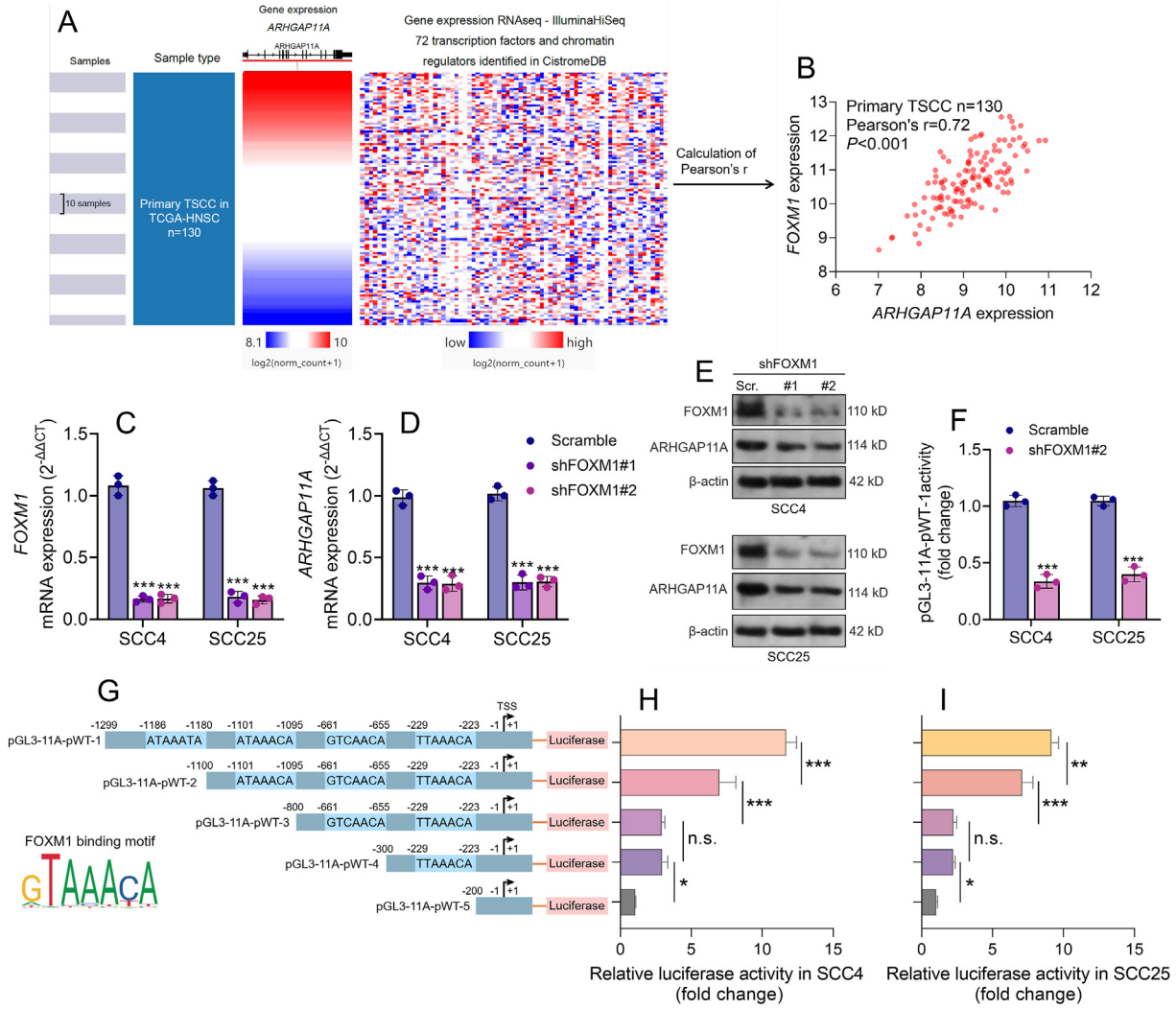

Figure 4 *ARHGAP11A* is transcriptionally activated by FOXM1 in tongue squamous cell carcinoma cells. **A.** A heatmap showing the general expression profile of *ARHGAP11A* and the candidate transcription factors and chromatin regulators with potential binding to the *ARHGAP11A* promoter region (within 10 kb before the transcription start site) in the primary tongue squamous cell carcinoma (TSCC) cases in TCGA-HNSC. **B.** A dot chart showing the correlation between *ARHGAP11A* and *FOXM1* in the primary TSCC cases. **C-E.** RT-qPCR (C–D) and western blotting (E) analyses were performed to check the expression of *FOXM1* and *ARHGAP11A* at the mRNA and protein levels in SCC4 and SCC25 cells 48 h after lentivirus-mediated *FOXM1* knockdown. **F.** Dual-luciferase assays were performed to check the relative luciferase activities of pGL3-11A-pWT-1 in SCC4 and SCC25 cells with or without *FOXM1* knockdown. **G.** A schematic diagram showing the design of recombinant pGL3-basic plasmids carrying integrated *ARHGAP11A* promoter region (pGL3-11A-pWT-1) and the truncated fragments. **H–I.** Dual-luciferase assays were performed to check the relative luciferase activities of pGL3-11A-pWT-1 and the truncated counterparts in SCC4 and SCC25 cells. n.s., not significant; **, $P < 0.01$; ***, $P < 0.001$.

Using JASPAR (https://jaspar.elixir.no/),[18] we checked the promoter region of *ARHGAP11A* and found four high-potential FOXM1 binding sites (red font, Supplementary Fig. 1). To evaluate FOXM1's effect on *ARHGAP11A* promoter activity, we constructed recombinant luciferase reporter plasmids containing either the full-length or truncated fragments of the *ARHGAP11A* promoter in the pGL3-basic plasmid (Fig. 4G). Knocking down endogenous *FOXM1* led to a significant reduction in luciferase activity from the pGL3-11A-WT1 construct in both SCC4 and SCC25 cells (Fig. 4F). Truncations at positions −229 to −233, −1101 to −1095, and −1186 to −1180 markedly diminished promoter activity, indicating that these sites likely represent the primary FOXM1 binding sites (Fig. 4G–I).

Discussion

Although *ARHGAP11A* overexpression and its association with malignant tumor behaviors and poor prognosis were observed in multiple types of cancer,[5,7–10] its functional involvement in OSCC is still unclear. By performing subgroup analysis using data from TCGA-HNSC, we found that

ARHGAP11A upregulation was associated with unfavorable OS in patients with TSCC and might be an independent prognostic indicator. These findings raise the possibility that ARHGAP11A could serve as a prognostic biomarker for TSCC and might be an oncogene. Subsequent *in vitro* and *in vivo* experiments supported this hypothesis, showing that *ARHGAP11A* silencing reduces the proliferation of TSCC cells and triggers G1 phase cell cycle arrest.

Functionally, ARHGAP11A is known to facilitate the hydrolysis of GTP-RhoA.[5,7] Consistent with this, our Western blot analysis showed that ARHGAP11A reduces the active GTP-bound form of RhoA without affecting the total RhoA protein levels in TSCC cells. Despite the observed tumor-suppressive effects following RHOA knockdown in TSCC cells, which include inhibited tumor growth, migration, and invasion,[21] *RHOA* expression is typically lower in TSCC tissues compared to adjacent normal tissues. Moreover, RHOA mutations are infrequent in HNSCC, with a prevalence of only 1.9%, suggesting that RHOA may not function as an essential oncogene in this context.[22,23]

RB1 is a tumor suppressor gene that encodes the RB protein, which regulates the cell cycle by controlling the transition from the G1 phase to the S phase.[24] When RB is phosphorylated by Cyclin-dependent kinases (CDKs), it becomes inactivated, leading to the release of E2F transcription factors that promote the expression of genes necessary for S phase entry and DNA replication.[24] p27 is a member of the Kip family of cyclin-dependent kinase inhibitors (CKIs) and functions as a regulator of cell cycle progression at G1.[25] It acts by attaching to and suppressing the function of Cyclin E-CDK2 or Cyclin D-CDK4 complexes, thereby playing a role in controlling the advancement of the cell cycle during the G1 phase. Cyclin E1 forms a complex with CDK2 which is crucial for the cell to transition from G1 to S phase of the cell cycle.[25] The cyclin E1-CDK2 complex phosphorylates RB, leading to the release of E2F and the transcription of genes needed for DNA replication.[25]

In TSCC, as in other cancers, the interplay between these molecules is crucial. The loss of regulatory control over the cell cycle allows cancer cells to multiply without the normal checks and balances.[26] TSCC cells often show alterations in the *RB1* pathway. When *RB1* function is lost or compromised, cells can bypass the G1 checkpoint, leading to uncontrolled cell division and tumorigenesis.[27] Similarly, reduced expression or inactivation of p27 is frequently seen in TSCC,[28] which can contribute to increased CDK activity and unregulated cell cycle progression. Higher levels of cyclin E1 can lead to increased phosphorylation of RB, overwhelming the cell's ability to regulate the G1-S transition, which can lead to increased proliferation and potentially contribute to the development and progression of TSCC.[29] Our results showed that *ARHGAP11A* knockdown decreased p-RB1 and cyclin E1 but restored p27 levels in SCC4 and SCC25 cells. These mechanisms help explain why *ARHGAP11A* knockdown slowed tumor cell growth and induced G1 arrest.

Since *ARHGAP11A* is aberrantly upregulated in TSCC, understanding how it is dysregulated can provide insights into the molecular pathogenesis of TSCC. Therefore, we further explored the transcription factors and confirmed that *ARHGAP11A* is transcriptionally activated by FOXM1 in TSCC. FOXM1 is a master transcriptional regulator that controls the expression of genes involved in cell proliferation, differentiation, DNA damage repair, and tissue homeostasis.[30] In cancers, FOXM1 is frequently overexpressed. Several mechanisms likely contribute to FOXM1 upregulation, including gene amplification (gain of chromosome 14), trancrioptional dysregulation (such ascis-acting elements such as E-boxes responsive to other transcription factors in the gene promoter), post-translational modifications (such as mRNAs), post-translational modifications (such as phosphorylation, ubiquitination, SUMOylation, acetylation and methylation) and activation by oncogenic signaling pathways.[31] Once overexpressed, FOXM1 acts as a master regulator, altering the transcriptional landscape in ways that promote hallmarks of cancer.[30] In TSCC, the upregulation of *FOXM1* was associated with enhanced proliferation, epithelial—mesenchymal transition, invasion, and migration,[32,33] failure of treatment in the early stages,[34] and radioresistance.[35] Our results demonstrate that one such FOXM1 transcriptional target in OSCC is ARHGAP11A. We found FOXM1 binds directly to the ARHGAP11A promoter to activate its expression. Therefore, *ARHGAP11A* is likely a part of a complex network of cell-cycle dysregulation in TSCC and its regulation by FOXM1 is one aspect of this network.

Overall, this study advances our understanding of the key molecular mechanisms governing TSCC pathogenesis. Further exploration of components of the FOXM1-ARHGAP11A pathway may worth of ongoing efforts to develop more effective targeted therapies for this aggressive malignancy. This study has provided evidence for the oncogenic role of ARHGAP11A in TSCC, with implications for cell cycle regulation and tumor growth. Furthermore, the regulatory relationship with FOXM1 opens new avenues for understanding the transcriptional networks in TSCC and could pave the way for novel therapeutic interventions.

Declaration of competing interest

The authors have no conflicts of interest relevant to this article.

Acknowledgments

No funding was received.

Appendix A. Supplementary data

Supplementary data to this article can be found online at https://doi.org/10.1016/j.jds.2024.02.015.

References

1. Johnson DE, Burtness B, Leemans CR, Lui VWY, Bauman JE, Grandis JR. Head and neck squamous cell carcinoma. *Nat Rev Dis Prim* 2020;6:92.
2. Leemans CR, Braakhuis BJ, Brakenhoff RH. The molecular biology of head and neck cancer. *Nat Rev Cancer* 2011;11:9—22.

3. Cancer Genome Atlas N. Comprehensive genomic characterization of head and neck squamous cell carcinomas. *Nature* 2015;517:576—82.
4. Song S, Cong W, Zhou S, et al. Small GTPases: structure, biological function and its interaction with nanoparticles. *Asian J Pharm Sci* 2019;14:30—9.
5. Lawson CD, Fan C, Mitin N, et al. Rho GTPase transcriptome analysis reveals oncogenic roles for Rho GTPase-activating proteins in basal-like breast cancers. *Cancer Res* 2016;76:3826—37.
6. Haga RB, Ridley AJ. Rho GTPases: regulation and roles in cancer cell biology. *Small GTPases* 2016;7:207—21.
7. Kagawa Y, Matsumoto S, Kamioka Y, et al. Cell cycle-dependent Rho GTPase activity dynamically regulates cancer cell motility and invasion in vivo. *PLoS One* 2013;8:e83629.
8. Lu S, Zhou J, Sun Y, et al. The noncoding rna hoxd-as1 is a critical regulator of the metastasis and apoptosis phenotype in human hepatocellular carcinoma. *Mol Cancer* 2017;16:125.
9. Chen S, Duan H, Xie Y, Li X, Zhao Y. Expression and prognostic analysis of Rho GTPase-activating protein 11A in lung adenocarcinoma. *Ann Transl Med* 2021;9:872.
10. Fan B, Ji K, Bu Z, et al. Arhgap11a is a prognostic biomarker and correlated with immune infiltrates in gastric cancer. *Front Mol Biosci* 2021;8:720645.
11. Goldman MJ, Craft B, Hastie M, et al. Visualizing and interpreting cancer genomics data via the Xena platform. *Nat Biotechnol* 2020;38:675—8.
12. Thul PJ, Akesson L, Wiking M, et al. A subcellular map of the human proteome. *Science* 2017;356.
13. Grant GD, Kedziora KM, Limas JC, Cook JG, Purvis JE. Accurate delineation of cell cycle phase transitions in living cells with PIP-FUCCI. *Cell Cycle* 2018;17:2496—516.
14. Parisi L, Bianchi MG, Ghezzi B, et al. Preparation of human primary macrophages to study the polarization from monocyte-derived macrophages to pro- or anti-inflammatory macrophages at biomaterial interface in vitro. *J Dent Sci* 2023;18:1630—7.
15. Sun L, Xing G, Wang W, Ma X, Bu X. Proliferation-associated 2G4 P48 is stabilized by malignant T-cell amplified sequence 1 and promotes the proliferation of head and neck squamous cell carcinoma. *J Dent Sci* 2023;18:1588—97.
16. Group NCRRGW. Animal research: reporting in vivo experiments: the ARRIVE guidelines. *J Physiol* 2010;588:2519—21.
17. Shen Y, Vignali P, Wang R. Rapid profiling cell cycle by flow cytometry using concurrent staining of dna and mitotic markers. *Bio Protoc* 2017;7:e2517.
18. Fornes O, Castro-Mondragon JA, Khan A, et al. Jaspar 2020: update of the open-access database of transcription factor binding profiles. *Nucleic Acids Res* 2020;48:D87—92.
19. Ghandi M, Huang FW, Jane-Valbuena J, et al. Next-generation characterization of the cancer cell line encyclopedia. *Nature* 2019;569:503—8.
20. Zheng R, Wan C, Mei S, et al. Cistrome data browser: expanded datasets and new tools for gene regulatory analysis. *Nucleic Acids Res* 2019;47:D729—35.
21. Yan G, Zou R, Chen Z, et al. Silencing rhoa inhibits migration and invasion through wnt/beta-catenin pathway and growth through cell cycle regulation in human tongue cancer. *Acta Biochim Biophys Sin* 2014;46:682—90.
22. Schaefer A, Der CJ. Rhoa takes the rhoad less traveled to cancer. *Trends Cancer* 2022;8:655—69.
23. Svensmark JH, Brakebusch C. Rho GTPases in cancer: friend or foe? *Oncogene* 2019;38:7447—56.
24. Mandigo AC, Tomlins SA, Kelly WK, Knudsen KE. Relevance of pRB loss in human malignancies. *Clin Cancer Res* 2022;28:255—64.
25. Matthews HK, Bertoli C, de Bruin RAM. Cell cycle control in cancer. *Nat Rev Mol Cell Biol* 2022;23:74—88.
26. Wu YH, Yu-Fong Chang J, Chiang CP, Wang YP. Combined evaluation of both wee1 and phosphorylated cyclin dependent kinase 1 expressions in oral squamous cell carcinomas predicts cancer recurrence and progression. *J Dent Sci* 2022;17:1780—7.
27. Hsu PJ, Yan K, Shi H, Izumchenko E, Agrawal N. Molecular biology of oral cavity squamous cell carcinoma. *Oral Oncol* 2020;102:104552.
28. Vallonthaiel AG, Singh MK, Dinda AK, Kakkar A, Thakar A, Das SN. Prognostic significance of cytoplasmic p27 in oral squamous cell carcinoma. *J Oral Pathol Med* 2016;45:475—80.
29. Sur S, Nakanishi H, Steele R, Zhang D, Varvares MA, Ray RB. Long non-coding RNA ELDR enhances oral cancer growth by promoting ILF3-cyclin E1 signaling. *EMBO Rep* 2020;21:e51042.
30. Zona S, Bella L, Burton MJ, Nestal de Moraes G, Lam EW. FOXM1: an emerging master regulator of DNA damage response and genotoxic agent resistance. *Biochim Biophys Acta* 2014;1839:1316—22.
31. Liao GB, Li XZ, Zeng S, et al. Regulation of the master regulator foxm1 in cancer. *Cell Commun Signal* 2018;16:57.
32. Yang H, Wen L, Wen M, et al. Foxm1 promotes epithelial-mesenchymal transition, invasion, and migration of tongue squamous cell carcinoma cells through a c-met/akt-dependent positive feedback loop. *Anti Cancer Drugs* 2018;29:216—26.
33. Roh V, Hiou-Feige A, Misetic V, et al. The transcription factor foxm1 regulates the balance between proliferation and aberrant differentiation in head and neck squamous cell carcinoma. *J Pathol* 2020;250:107—19.
34. Thangaraj SV, Shyamsundar V, Krishnamurthy A, Ramshankar V. Deregulation of extracellular matrix modeling with molecular prognostic markers revealed by transcriptome sequencing and validations in oral tongue squamous cell carcinoma. *Sci Rep* 2021;11:250.
35. Takeshita H, Yoshida R, Inoue J, et al. Foxm1-mediated regulation of reactive oxygen species and radioresistance in oral squamous cell carcinoma cells. *Lab Invest* 2023;103:100060.